Feedback Control of Dissipative PDE Systems using Adaptive Model Reduction

Amit Varshney, Sivakumar Pitchaiah, and Antonios Armaou
Dept. of Chemical Engineering, The Pennsylvania State University, University Park, PA 16802

DOI 10.1002/aic.11770
Published online February 20, 2009 in Wiley InterScience (www.interscience.wiley.com).

The problem of feedback control of spatially distributed processes described by highly dissipative partial differential equations (PDEs) is considered. Typically, this problem is addressed through model reduction, where finite dimensional approximations to the original infinite dimensional PDE system are derived and used for controller design. The key step in this approach is the computation of basis functions that are subsequently utilized to obtain finite dimensional ordinary differential equation (ODE) models using the method of weighted residuals. A common approach to this task is the Karhunen-Loève expansion combined with the method of snapshots. To circumvent the issue of a priori *availability of a sufficiently large ensemble of PDE solution data, the focus is on the recursive computation of eigenfunctions as additional data from the process becomes available. Initially, an ensemble of eigenfunctions is constructed based on a relatively small number of snapshots, and the covariance matrix is computed. The dominant eigenspace of this matrix is then utilized to compute the empirical eigenfunctions required for model reduction. This dominant eigenspace is recomputed with the addition of each snapshot with possible increase or decrease in its dimensionality; due to its small dimensionality the computational burden is relatively small. The proposed approach is applied to representative examples of dissipative PDEs, with both linear and nonlinear spatial differential operators, to demonstrate its effectiveness of the proposed methodology.*
 AIChE J, 55: 906–918, 2009
Keywords: control of PDEs, model reduction, distributed parameter systems, process control

Introduction

Most of the processes relevant to the chemical process industry necessitate the consideration of transport phenomena (fluid flow, heat and mass transfer) often coupled with chemical reactions. Examples range from reactive distillation in petroleum processing to plasma enhanced chemical vapor deposition, etching and metallorganic vapor phase epitaxy (MOVPE) in semiconductor manufacturing. Mathematical descriptions of these transport-reaction processes can be derived from dynamic conservation equations and usually involve highly dissipative (typically parabolic) partial differential equation (PDEs) systems. The problem of feedback control of such processes is nontrivial owing to these spatially distributed mathematical descriptions.

A standard approach to feedback control of these systems involves the formulation of a finite dimensional approximation to the original infinite dimensional system by spatial discretization using Galerkin's method.[1–3] This yields a system of ordinary differential equations (ODEs) that describes the dominant/long-time dynamics of the PDEs, which can be subsequently utilized to design feedback controllers.[4,5] However, a drawback of this approach is that typically a large number of modes are required to accurately capture the dynamics of the PDE. Consequently, the dimensionality of the ODE approximation is large which leads to complex controller design and high-dimensionality of the resulting controllers.

To circumvent this problem, the concepts of inertial manifold (IM)[6,7] and approximate inertial manifold (AIM)[8–10] were used to derive lower order differential algebraic

Correspondence concerning this article should be addressed to A. Armaou at armaou@engr.psu.edu.

equation (DAE) systems, which capture the dominant dynamics of quasi-linear PDEs (systems having linear spatial differential operators and nonlinear terms that enter in an additive fashion). The derived DAE systems were further used for the synthesis of nonlinear low-dimensional output feedback controllers which enforce stability and output tracking in the closed-loop system. However, the aforementioned procedures cannot be directly applied to systems which have nonlinear spatial differential operators or to problems defined over irregular spatial domains (e.g., chemical reactors with complex geometry), since the eigenvalue-eigenfunction problem of the spatial operator for these systems cannot be analytically solved in general, and it, is, thus, difficult to derive the basis functions to expand the solution of the PDE system. In order to overcome this issue studies have focussed on linearization[1] of the spatial nonlinear operator around a steady state, while designing linear-quadratic optimal feedback control laws. However, the basis functions obtained through this procedure can be used only in the neighborhood of the steady state where this linearization takes place. Alternatively, optimal basis functions were derived for nonlinear PDE systems using Karhunen-Loève expansion (KLE), and the calculated basis functions were used in the method of weighted residuals.[11,12]

However, KLE involves the solution to an eigenvalue-eigenfunction problem of an integral operator; this is in general, a computationally expensive task. This issue was addressed in the method of snapshots,[13] a numerical procedure that reduces the computational cost involved in the above eigenvalue problem. This method has been extensively utilized to "empirically" compute the eigenfunctions of nonlinear PDEs using an ensemble of solution data obtained either through experimental observations or from detailed numerical simulations. KLE along with the method of snapshots has been used extensively in model reduction,[14] optimization[15–17] and control[18–20] of distributed processes. The shape of the empirical eigenfunctions accounts for the spatiotemporal behavior of the given PDE system which, therefore, allows computation of finite-dimensional lower-order models. This approach, however, relies on the a priori availability of a large ensemble of PDE solution data (snapshots) in which all the possible spatial modes have been excited. Unfortunately, no well defined methodology exists for generating such an ensemble.

A promising procedure to circumvent this issue, specifically for controller design, is to initially compute the eigenfunctions using the available ensemble of snapshots and continuously refine the eigenfunctions online as more snapshots of the process become available. The computation of the empirical eigenfunctions requires the solution of the eigenvalue problem of the covariance matrix of the snapshots, which might become expensive for online computations. In this article, we describe a procedure to recursively compute the empirical eigenfunctions of a given PDE system. The approach is based on the computation of an approximation of the eigenspace of the covariance matrix corresponding to its significant eigenvalues. This dominant eigenspace is updated recursively as new snapshots from the process are added to the ensemble, simultaneously increasing or decreasing its dimensionality if required. We maintain that as long as the dimensionality of the dominant eigenspace remains small, the computational burden for updating the dominant eigenspace remains small and can be easily performed online. The focus of this procedure is the derivation of low-order models specifically tailored for the design of feedback controllers and observers for distributed processes. Following the derivation of the reduced-order model, nonlinear model based feedback controllers are designed. We evaluate the effectiveness of the proposed approach numerically through a representative example of a diffusion-reaction process.

Mathematical preliminaries

We focus on the problem of feedback control of spatially distributed processes described by highly dissipative PDEs with the following state-space description

$$\begin{aligned} \frac{\partial x}{\partial t} &= \mathcal{A}(x) + b(z)u + f(x) \\ y_c &= \int_\Omega c(z)x\,dz \\ y_m &= \int_\Omega s(z)x\,dz \end{aligned} \tag{1}$$

subject to the mixed-type boundary conditions

$$q\left(x, \frac{dx}{d\eta}, \ldots, \frac{d^{n_o-1}x}{d\eta^{n_o-1}}\right) = 0 \text{ on } \Gamma \tag{2}$$

and the following initial condition

$$x(z,0) = x_0(z) \tag{3}$$

In the aforementioned PDE system, $x(z,t) \in \mathbb{R}^n$ denotes the vector of state variables, $y_c \in \mathbb{R}^k$ denotes the vector of controlled outputs, t is the time, $y_m \in \mathbb{R}^{n_{mo}}$ denotes the vector of measured outputs, $z \in \Omega \subset \mathbb{R}$ is the spatial coordinate, Ω is the domain of definition of the process, and Γ is its boundary. $\mathcal{A}(x)$ is a highly dissipative, possibly nonlinear, spatial differential operator of order n_o, where n_o is an even number; $f(x)$ is a nonlinear vector function, which is assumed to be sufficiently smooth with respect to its arguments, $c(z)$ is a known smooth vector function of z, which is determined by the desired performance specifications in the domain Ω, and $s(z)$ is a known smooth vector function of z, which is determined by the location and type of measurement sensors (e.g., point or distributed sensing), $u = [u_1, u_2, \ldots, u_k] \in \mathbb{R}^k$ denotes the vector of manipulated inputs, $b(z) \in \mathbb{R}^{n\times k}$ is a known smooth matrix function of z of the form $[b_1(z), b_2(z), \ldots, b_k(z)]$, where $b_i(z)$ describes how the i^{th} control action $u_i(t)$ is distributed in the spatial domain Ω, $q(x, (dx/d\eta), \ldots, (d^{n_0-1}x/d\eta^{n_0-1}))$ is a nonlinear vector function which is assumed to be sufficiently smooth, $\frac{dx}{d\eta}|_\Gamma$ denotes the derivative in the direction perpendicular to the boundary, and $x_0(z)$ is a smooth vector function of z. We note that in the case of point actuation which influences the system at z_0 (i.e., $b_i(z)$ is equal to $\delta(z - z_0)$, where $\delta(\cdot)$ is the standard Dirac function), we approximate the function $\delta(z - z_0)$ by the finite value $1/2\varepsilon$ in the interval $[z_0 - \varepsilon, z_0 + \varepsilon]$ (where ε is a small positive real number) and zero elsewhere in the domain. We assume that for a given set of initial and boundary conditions the system of Eqs. 1–3 has a unique solution.

We define the inner product and norm in $L_2[\Omega]$, where $L_2[\Omega]$ is the space of square integrable functions defined in Ω, as follows

$$(\phi_1, \phi_2) = \int_\Omega \phi_1^*(z)\phi_2(z)dz, ||\phi_1||_2 = (\phi_1, \phi_1)^{1/2} \quad (4)$$

where ϕ_1, $\phi_2 \in L_2[\Omega]$ and * denotes the complex conjugate transpose.

We also define the Lie derivative of the scalar function $h_i(x)$ with respect to the vector function $f(x)$ as $L_f h_i(x) = (((\partial h_i(x)/\partial x) f(x)) \cdot L_f^k h_i(x)$ denotes the k-th order Lie derivative, and $L_g L_f^k h_i(x)$ denotes the mixed Lie derivative.

Problem Formulation and Solution Methodology

In this section, our objective is to present an outline of the steps of the adaptive model reduction and control methodology for processes that are described by the system of Eqs. 1–3. The control problem is formulated as the one of deriving a feedback control law $u(t) = G(x(t))$, such that the closed-loop system is stabilized at a desired set point. Without loss of generality, we assume the setpoint is $x(z, t) = 0$. The steps of the proposed methodology to achieve the above task are:

1. Initially generate an ensemble of solution data either through experimental observations or from detailed numerical simulations.
2. Analyze the PDE solution data and obtain the basis functions using KLE and use the method of weighted residuals to construct a finite-dimensional approximation of the PDE.
3. Design a state feedback controller based on the finite dimensional approximation.
4. Recursively modify the eigenfunctions and the finite dimensional approximation as new process measurements become available. This step may require addition or deletion of eigenfunctions. Redesign the feedback controller based on the modified finite dimensional approximation.

A closed-loop diagram illustrating the different steps of the developed methodology is presented in Figure 1. We note that the initial data required for evaluating the eigenfunctions can be obtained either experimentally (by allowing the process to evolve with no control action for a short period of time), or from previously obtained historical data, or numerically by using offline simulation packages for PDE systems such as Fluent and Comsol and, subsequently, evaluating the simulation results. The following subsections are intended to describe each of the above steps in detail.

Computation of empirical eigenfunctions using KLE

In this section, we use the off-line solution data of the system of Eq. 1 to construct the basis functions necessary for the derivation of finite dimensional ODE models. KLE is a procedure used to compute an optimal set of empirical eigenfunctions from an appropriately constructed set of solutions of the PDE system of Eq. 1. In general (but not in this method; see remark 1), the ensemble of solutions is constructed by computing the solutions of the PDE system of Eq. 1 for different values of $u(t)$, and different initial conditions.[14,15,21]

Application of KLE to this ensemble of data provides an orthogonal set of basis functions (known as empirical eigenfunctions) for the representation of the ensemble, as well as

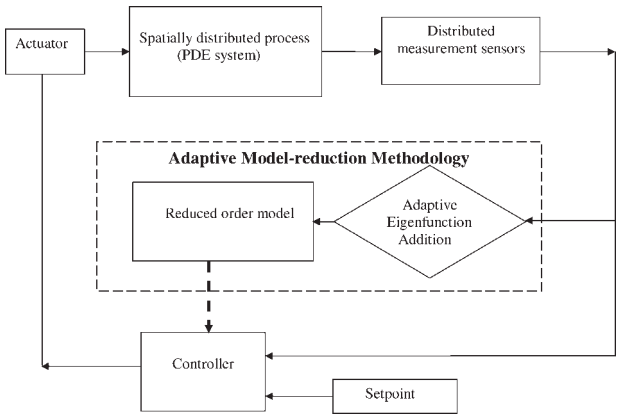

Figure 1. Process operation block diagram under proposed controller design.

a measure of the relative contribution of each basis function to the total energy (mean-square fluctuation) of the ensemble. A truncated series representation of the ensemble data in terms of these dominant basis functions has a smaller mean-square error than a representation by any other basis of the same dimension.[22] Therefore, KLE yields the most efficient way for computing the basis functions (corresponding to the largest empirical eigenvalues) which capture the dominant patterns of the ensemble. Let v_κ denote the snapshot of the system available at time t_κ, and let the total number of snapshots available be K. We will briefly present the key features of KLE. The reader may refer to[13,22,23] for a detailed presentation and analysis of the KLE.

We define the ensemble average as $\langle \Psi_\kappa \rangle := \frac{1}{K}\sum_{\kappa=1}^{K} \Psi_\kappa(z)$, where Ψ_κ denotes the snapshot of a vector quantity at time t_κ (nonuniform sampling of the snapshots and weighted ensemble averages can be also considered[14]). The issue is how to obtain the most typical or characteristic spatial profile (in a sense that will become clear below) $\phi(z)$ from these snapshots $\{v_\kappa\}$. Mathematically, this problem can be posed as the one of obtaining a function $\phi(z)$ that maximizes the following objective function

$$\begin{aligned} &\text{Maximize} \frac{\langle (\phi, v_\kappa)^2 \rangle}{(\phi, \phi)} \\ &s.t. (\phi, \phi) = 1,\ \phi \in L^2([\Omega]) \end{aligned} \quad (5)$$

which, in other words, implies that the projection of v_κ on the subspace spanned by $\phi(z)$ captures the maximum energy contained in these snapshots. The constraint $(\phi, \phi) = 1$ is imposed to ensure that the function, $\phi(z)$, computed as a solution of the earlier maximization problem, is unique. An alternative way to express the constrained optimization problem of Eq. 5 is to solve the perturbation problem for ϕ

$$\frac{dL(\phi + \delta\varphi)}{d\delta}(\delta = 0) = 0, (\phi, \phi) = 1 \quad (6)$$

where $L = \langle (\phi, v_\kappa)^2 \rangle - \lambda((\phi, \phi) - 1)$ is the corresponding Lagrangian functional, and δ is a real number.

Using the definitions of inner product and ensemble average, $(dL(\phi+\delta\varphi)/d\delta)(\delta=0)$ can be computed from the following expression

$$\frac{dL(\phi+\delta\varphi)}{d\delta}(\delta=0) = \int_\Omega \left(\left\{ \int_\Omega \langle v_\kappa(z) v_\kappa(\bar{z}) \rangle \phi(z) dz \right\} - \lambda\phi(\bar{z}) \right) \Gamma(\bar{z}) d\bar{z} \quad (7)$$

Since $\Gamma(\bar{z})$ is an arbitrary function, the necessary conditions for optimality take the form

$$\int_\Omega \langle v_\kappa(z) v_\kappa(\bar{z}) \rangle \phi(z) dz = \lambda\phi(\bar{z}),\ (\phi,\phi)=1 \quad (8)$$

Introducing the two-point correlation function

$$K(z,\bar{z}) = \langle v_\kappa(z) v_\kappa(\bar{z}) \rangle = \frac{1}{K}\sum_{\kappa=1}^{K} v_\kappa(z) v_\kappa(\bar{z}) \quad (9)$$

and the integral operator

$$R := \int_\Omega K(z,\bar{z}) d\bar{z} \quad (10)$$

the optimality condition of Eq. 8 reduces to the following eigenvalue-eigenfunction problem of the integral operator

$$R\phi = \lambda\phi \Rightarrow \int_\Omega K(z,\bar{z})\phi(\bar{z}) d\bar{z} = \lambda\phi(z) \quad (11)$$

The computation of the solution of the aforementioned integral eigenvalue problem is, in general, a very expensive computational task. To circumvent this problem, Sirovich, in 1987, introduced the method of snapshots.[13] The central idea of this technique is to assume that the requisite eigenfunction $\phi(z)$, can be expressed as a linear combination of the snapshots i.e.

$$\phi(z) = \sum_k \psi^k v_k(z) \quad (12)$$

where ψ^k denotes the kth element of vector ψ.

Substituting the above expression for $\phi(z)$ on Eq. 11, we obtain the following eigenvalue problem

$$\int_\Omega \frac{1}{K}\sum_{\kappa=1}^{K} v_\kappa(z) v_\kappa(\bar{z}) \sum_{k=1}^{k} \psi^k v_k(\bar{z}) d\bar{z} = \lambda \sum_{k=1}^{K} \psi^k v_k(z) \quad (13)$$

Defining the (κ, k)th element $C_K^{\kappa k}$ of matrix C_K as

$$C_K^{\kappa k} := \frac{1}{K}\int_\Omega v_\kappa(\bar{z}) v_k(\bar{z}) d\bar{z} \quad (14)$$

the eigenvalue problem of Eq. 13 can be equivalently written as

$$C_K\psi = \lambda\psi \quad (15)$$

The solution of the above eigenvalue problem (obtained by utilizing standard methods from linear algebra[24]) yields K eigenvectors $\psi_1, \psi_2, \ldots, \psi_K$, which can be used in Eq. 12 to construct K eigenfunctions $\phi_\kappa(z)$, $\kappa = 1, \ldots, K$. By construction, matrix C_K is symmetric and positive semidefinite, and thus, its eigenvalues, λ_κ, $\kappa = 1, \ldots, K$, are real and, non-negative. The relative magnitude of the eigenvalues represents a measure of the fraction of the "energy" embedded in the ensemble captured by the corresponding eigenfunctions. We order the calculated empirical eigenfunctions such that

$$\lambda_1 > \lambda_2 > \cdots > \lambda_K \quad (16)$$

Furthermore, the resulting eigenfunctions form an orthonormal set, i.e.

$$\int_\Omega \phi_i(z)\phi_j(z) dz = 0, i \neq j \text{ and } \int_\Omega \phi_i(z)\phi_i(z) dz = 1 \quad (17)$$

Iterative methods, such as Krylov subspace methods,[24] can be used to reduce the computational cost associated with the computation of the eigenvalues and eigenfunctions.

Remark 1. Since we are recursively updating the eigenfunctions as snapshots arrive, it should be noted that we need not perform an exhaustive sampling of the state-space of the PDE by evolving the system from a number of different initial conditions, and for different values of actuation during ensemble generation.

Derivation of finite dimensional approximations using method of weighted residuals

We employ the identified empirical eigenfunctions to derive finite-dimensional approximations of the infinite-dimensional PDE system of Eq. 1, by using the method of weighted residuals. To simplify the notation, without loss of generality we consider the system of Eq. 1 with $n = 1$. In principle, $x(z, t)$ can be represented as an infinite weighted sum of a complete set of basis functions $\phi_k(z)$. We can obtain an approximation $x_N(z, t)$, by truncating the series expansion of $x(z, t)$ up to order N, as follows

$$x_N(z,t) = \sum_{k=1}^{N} a_k(t)\phi_k(z) \xrightarrow{N\to\infty} x(z,t) = \sum_{k=1}^{\infty} a_k(t)\phi_k(z) \quad (18)$$

where $a_k(t)$ is a time-varying coefficient called the mode of the system.

Substituting the expansion of Eq. 18 into Eq. 1, multiplying the PDE with the weighting functions, $\omega(z)$, and integrating over the entire spatial domain (i.e., taking inner product in $L_2[\Omega]$ with the weighting functions), the following N-th order system of ODEs is obtained

$$-\sum_{k=1}^{N} \dot{a}_k \left(\int_\Omega \omega(z)\phi_k(z) dz \right) + \int_\Omega \omega(z) \mathcal{A}\left(\sum_{k=1}^{N} a_k(t)\phi_k(z) \right) dz + \int_\Omega \omega(z) b(z) u dz + \int_\Omega \omega(z) f\left(\sum_{k=1}^{N} a_k(t)\phi_k(z) \right) dz = 0, \quad v = 1, \ldots, N \quad (19)$$

The weighting functions in the above equation determine the type of weighted residual method being used. When the weighting functions are the basis functions, $\omega(z) = \phi(z)$, the method of weighted residuals reduces to Galerkin's method.

In the proposed methodology, since we are using empirical eigenfunctions for this expansion we slightly abuse the terminology, and we continue to call this Galerkin's method. The resulting ODE system can be written compactly in the form

$$\dot{a} = \mathcal{F}(a) + \mathcal{G}u \tag{20}$$

where $a \in \mathbb{R}^N$ are now called empirical eigenmodes, and $\mathcal{F}$, $\mathcal{G}$ are vector and matrix functions of appropriate dimensions defined in Eq. 22 below.

Controller design using feedback linearization

In this section, we employ feedback linearization to design state feedback controllers for the system of Eq. 1, based on the representation of Eq. 20. To simplify the development, we represent the system in the following compact form

$$\begin{aligned} \dot{a} &= \mathcal{F}(a) + \mathcal{G}u = \mathcal{F}(a) + \sum_{i=1}^{k} \mathcal{G}_i u_i, \\ y_m &= \int_\Omega s(z)x\,dz, \\ y_{c,i} &= h_i(a),\ i = 1, \ldots, k \end{aligned} \tag{21}$$

where

$$\begin{aligned} \mathcal{F}(a) &= \int_\Omega \phi(z)\mathcal{A}\left(\sum_{k=1}^{N} a_k(t)\phi_k(z)\right)dz \\ &\quad + \int_\Omega \phi(z) f\left(\sum_{k=1}^{N} a_k(t)\phi_k(z)\right)dz \\ \mathcal{G}_i &= \int_\Omega \phi(z) b_i(z)dz \\ h_i(a) &= \int_\Omega c^i(z)x dz \end{aligned} \tag{22}$$

where k is the number of manipulated inputs, u_i is the i^{th} manipulated input, y_m is the measured output vector, $\mathcal{S}$ denotes the measurement sensor shape function, and $y_{c,i}$ is the i^{th} controlled output. We assume that the relative degree r_i of the system of Eq. 21 is well defined for all values of a.[25]

We use feedback linearization to design state feedback controllers which have the following general form

$$u = p(a) + Q(a)\hat{v} \tag{23}$$

where $p(a)$ is a smooth vector function, $Q(a)$ is a smooth matrix, and $\hat{v} \in \mathbb{R}^k$ is the constant reference input vector. Based on the relative degrees of the system of Eq. 20, we assign the following closed-loop behavior to the controlled outputs $y_{c,i}$

$$\sum_{i=1}^{k}\sum_{j=0}^{r_i} \beta_{ij}\frac{d^j y_{c,i}}{dt^j} = \hat{v} \tag{24}$$

The characteristic matrix of the system Eq. 21

$$C_0(a) = \begin{bmatrix} L_{\mathcal{G}_1}L_{\mathcal{F}}^{r_1-1}h_1(a) & \cdots & L_{\mathcal{G}_1}L_k^{r_1-1}h_1(a) \\ L_{\mathcal{G}_1}L_{\mathcal{F}}^{r_1-1}h_2(a) & \cdots & L_{\mathcal{G}_1}L_k^{r_2-1}h_2(a) \\ \vdots & \vdots & \vdots \\ L_{\mathcal{G}_1}L_{\mathcal{F}}^{r_1-1}h_l(a) & \cdots & L_{\mathcal{G}_1}L_k^{r_1-1}h_l(a) \end{bmatrix}$$

is assumed to be invertible (i.e., $det(C_0(a)) \neq 0$). Eq. 21 can be used to derive state feedback controller (of the form given by Eq. 23) that guarantee output behavior as described by Eq. 24.[25] The explicit form of the controller is:

$$u = \{[\beta_{1r_1} \ldots \beta_{kr_k}]C_0(a)\}^{-1}\left\{\hat{v} - \sum_{i=1}^{k}\sum_{j=0}^{r_i}\beta_{ij}L_f^j h_i(a)\right\} \tag{25}$$

The proof of the closed-loop properties of the proposed controller can be found in[25] and are omitted for brevity.

Recursive update of empirical eigenfunctions

The original KLE algorithm requires *a priori* availability of a sufficiently large ensemble of PDE solution data to compute empirical eigenfunctions. However, in practice, it is difficult to generate such an ensemble so that all possible dominant spatial modes are appreciably contained within the corresponding snapshots. The resulting eigenfunctions, therefore, are representative of the corresponding ensemble only. During closed-loop simulation, situations may arise when the existing eigenfunctions fail to accurately represent the dynamics of the PDE system.

One possible solution is to continue augmenting the ensemble of snapshots, and then recomputing the eigenfunctions as more information regarding the process becomes available. However, this would require the solution of the eigenvalue-eigenvector problem of Eq. 15, which may become computationally expensive, and hence, unsuitable for online computations as the process evolves. Furthermore, while we are traversing different regions of the state-space during the process evolution, old snapshots may not contain pertinent information of the process behavior in the local region.

To circumvent the latter problems, we propose an algorithm that allows for recursive update of empirical eigenfunctions *once new measurements from the process become available*. Let us define ε as the percentage energy of the ensemble captured by dominant eigenfunctions. The proposed algorithm is based on the partition of the eigenspace of the covariance matrix into two subspaces; the dominant one containing the modes which capture at least ε percent of energy in the ensemble (denoted as $\mathbb{P}$), and the orthogonal complement to $\mathbb{P}$ containing the rest of the modes (denoted as $\mathbb{Q}$). Such a partition is possible due to the fact that the dominant dynamics of highly dissipative PDEs are finite (typically small) dimensional.[6] The orthonormal basis for the subspace $\mathbb{P}$ is recursively updated upon the arrival of new snapshots, possibly by increasing or decreasing the size of the basis if required and by maintaining the accuracy of basis by performing orthogonal power iteration, while the orthonormal basis for $\mathbb{Q}$ can be computed from the fact that $\mathbb{Q}$ is the orthonormal complement of $\mathbb{P}$. We maintain that the extra work required for the aforementioned process is small as

long as the dimension of $\mathbb{P}$ is small (this amounts to choosing an appropriate value for ε).

As defined in the subsection about KLE, C_K denotes the covariance matrix obtained from K snapshots. We assume that out of K possible eigenvectors of C_K, m have the corresponding eigenvalues such that $\sum_{i=1}^{m} \lambda_i / \sum_{i=1}^{K} \lambda_i \geq \frac{\varepsilon}{100}$; m eigenmodes of C_K capture ε percent of energy in the ensemble. An orthonormal basis for the subspace $\mathbb{P}$ can be obtained as

$$Z = [\psi_1, \psi_2, \ldots, \psi_m], Z \in \mathbb{R}^{K \times m} \tag{26}$$

where $\psi_1, \psi_2, \ldots, \psi_m$ denote the eigenvectors of C_K that correspond to the eigenvalues $\lambda_1, \lambda_2, \ldots, \lambda_m$. Note that the eigenfunctions computed by using these eigenvectors in Eq. 12 capture the dominant dynamics of the PDE system of Eq. 1. The orthogonal projection operators P and Q onto subspaces $\mathbb{P}$ and $\mathbb{Q}$ can be computed as

$$P = ZZ^T, Q = I - ZZ^T \tag{27}$$

where I denotes the identity matrix of dimension K. Our task is to obtain the new basis Z, as new snapshots of the process become available. The algorithm outlined in the following section computes an approximation to Z without requiring the solution of the eigenvalue-eigenvector problem of the covariance matrix (Eq. 15). We assume that during each step at most one eigenmode joins the subspace $\mathbb{P}$. We also assume that the process changes slowly enough so that the appearance of new patterns is captured by the snapshots. The algorithm requires the dimensionality of the covariance matrix to remain constant, which we achieve by discarding the oldest snapshot from the ensemble.

As a new snapshot from the process becomes available, the subspace $\mathbb{P}$ may change in the following three ways.

- The dimension of the dominant subspace $\mathbb{P}$ may increase i.e., one mode corresponding from $\mathbb{Q}$ becomes necessary to capture the desired percentage of energy in the ensemble.
- Some of the eigenmodes of the subspace $\mathbb{P}$ may no longer be necessary to capture the required ε percent of the energy. In this case, the basis Z should be updated, and its dimension should be simultaneously decreased.
- The dimensionality of $\mathbb{P}$ remains unchanged, however, the basis Z needs to be updated in order to account for the newly added snapshot.

A flow chart illustrating the aforementioned steps is presented in Figure 2. In the following subsections, the earlier steps are explained in detail.

Increasing the Size of the Basis. In this section, we consider the case when one eigenmode of subspace $\mathbb{Q}$ becomes dominant as a new snapshot is added, in the sense that the associated eigenfunction becomes necessary to accurately describe the ensemble of solutions. The eigenmode thus becomes an element of subspace $\mathbb{P}$ and leaves $\mathbb{Q}$. To monitor this event we employ the following lemma.

Lemma 1: *The set of eigenvalues of $c_q = QC_KQ$ is the subset of eigenvalues of C_K that correspond to the eigenmodes which belong to subspace $\mathbb{Q}$.*

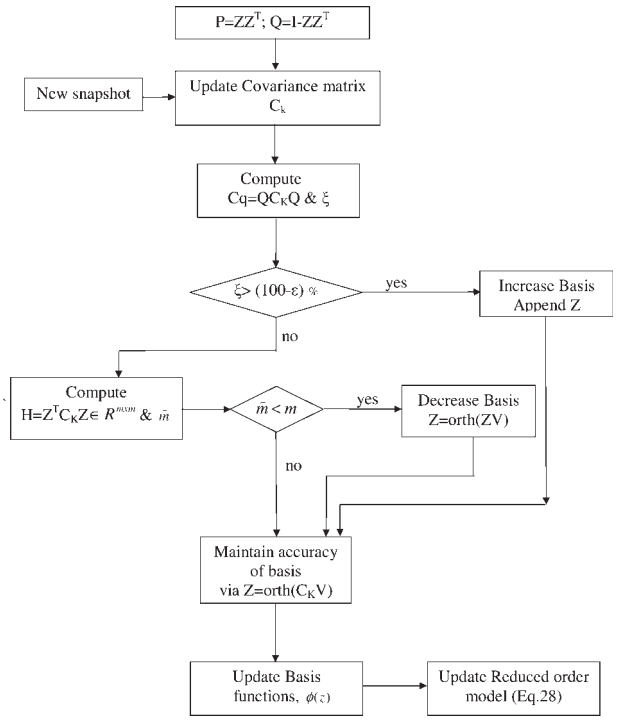

Figure 2. Flow chart of adaptive eigenfunction refinement and adaptive model reduction methodology.

See Appendix A for proof.

We, thus, monitor the percentage contribution of the dominant eigenvalue of $c_q = QC_KQ$, namely λ_{m+1} towards the total energy of the ensemble. We define the percentage contribution of λ_{m+1} as

$$\xi = \frac{\lambda_{m+1}}{\sum_{i=1}^{m+1} \lambda_i} \tag{28}$$

If ξ increases to more than $(100 - \varepsilon)$ percent we append Z, the basis of subspace $\mathbb{P}$, with the corresponding eigenvector (We note that the eigenvalues $\lambda_i \; \forall \; i = 1, \ldots, m$ can be computed by solving a small eigenvalue problem, see next subsection for details). We find the dominant eigenspace of c_q using the following power iteration

$$q^{(v+1)} \approx (c_q)^v q^{(0)} \tag{29}$$

The aforementioned iteration then produces iterates that asymptotically lie in the dominant eigenspace of c_q, provided the initial iterate $q^{(0)}$ has a nonzero component in that direction. The dominant eigenvalue of c_q can be computed as

$$\lambda_{m+1} = (q^c)^T c_q q^c \tag{30}$$

where q^c is the converged solution of the power iteration Eq. 29. The new eigenvector then becomes part of

$$Z = [\psi_1, \psi_2, \ldots, \psi_m, \psi_{m+1}], Z \in \mathbb{R}^{K \times m+1}$$

and its eigenvalue gets added to the dominant subspace $\mathbb{P}$. Consequently, the dimension of the subspace $\mathbb{P}$ is increased by one.

Decreasing the Size of the Basis. As new snapshots are added and old snapshots are eliminated from the ensemble, the dominant eigenspace of C_K continuously changes. Power iteration in the previous section identifies scenarios when one of the eigenmodes becomes dominant. However, it is likely that during the process some of the eigenmodes, in subspace $\mathbb{P}$, may no longer be necessary to capture the desired percentage of energy. In such cases, it is required to decrease the size of basis Z such that it spans the dominant eigenspace only. To test whether it is required to decrease the size of the basis we introduce the following $m \times m$ matrix

$$H = Z^T C_K Z, \quad H \in \mathbb{R}^{m \times m} \tag{31}$$

The eigenvalues of H correspond to the first m dominant eigenvalues of C_K. They can be computed with little computational effort as long as m remains small. If only $\hat{m}$, with $\hat{m} < m$, eigenvalues of H are dominant (in a sense that only $\hat{m}$ eigenmodes are required to capture ε percent of energy of the ensemble), then span$\{ZV\}$ provides a good approximation to the dominant eigenspace of C_K, where the basis $V \in \mathbb{R}^{m \times \hat{m}}$ is obtained from the eigenvectors of H corresponding to its $\hat{m}$ dominant eigenvalues. Hence, the step

$$Z = \text{orth}(ZV) \tag{32}$$

where orth$(\cdot)$ denotes Gram-Schmidt orthonormalization, automatically reduces the size of the basis whenever required.

Maintaining the Accuracy of the Basis. During the process evolution it may become apparent that even though the basis dimensionality remains the same, there is an increase in the error between the new snapshots and the projection identified using the "old" basis functions. The following one step orthogonal power iteration is performed in order to maintain the accuracy of the basis after each addition of a snapshot

$$\mathrm{Z} = \text{orth}(C_K \mathrm{Z}) \tag{33}$$

Remark 2. We note that the orthogonal projections P and Q should satisfy $QC_KP = 0$ (a result which follows from the fact that P is an orthogonal projector, see Appendix A). Hence, the accuracy of the basis can be also evaluated by computing the matrix $\mathcal{E} = (I - ZZ^T)C_K(ZZ^T)$.

Model Reduction and Controller Reconfiguration. Based on the new values of Z, we now compute the revised eigenfunctions $\phi_1, \phi_2, \ldots, \phi_m$ using (Eq. 12)

$$\phi(z) = \sum_k \psi^k v_k(z)$$

Using these eigenfunctions, we refine our reduced-order model

$$\dot{a} = \mathcal{F}(a) + \mathcal{G}u$$

and reconfigure the controller (Eq. 25) using the updated reduced-order model. This step assures that the reduced-order model captures new trends that appear when the process traverses through variable state space during closed-loop operation.

Remark 3. We note that the availability of a process model is assumed throughout this work. The fine point which separates this method from system identification and adaptive control literature is the fact that the process dynamic model is accurately known and the system state is accurately measured at all times. The focus of this work is to recursively update the reduced-order model of Eq. 21, computed initially based on the available process model, as the process states move through different regions in the state-space by recursively updating the empirical eigenfunctions using the methodology presented in this section.

Since the objective is to control the closed loop process and the process model is accurately known, there is no need to excite the process to achieve stabilization. The concepts used to recursively update the basis functions (e.g., the percentage contribution ζ, of the dominant eigenvalue of c_q) do not require the system to be persistently excited and can be computed from the covariance matrix C_K, obtained from measurements of the entire process state. When the covariance matrix stops providing the controller with relevant information (which can be measured by the value of the largest eigenvalue) the re-evaluation of the empirical eigenfunctions is suspended.

Application to Diffusion-Reaction Process

Linear spatial operator

In this section, we apply the proposed adaptive model reduction and control methodology to a typical diffusion-reaction process that exhibits nonlinear dynamic behavior. Specifically, we consider an elementary exothermic reaction A $\rightarrow$ B taking place on a thin catalytic rod. The temperature of the rod is adjusted by means of an actuator located along the length of the rod. Assuming that the reactant A is present in excess, the spatial profile of the dimensionless temperature of the rod is described by the following parabolic PDE

$$\frac{\partial x}{\partial t} = \frac{\partial^2 x}{\partial z^2} + \beta_T(e^{-\gamma/(1+x)} - e^{-\gamma}) + \beta_U(b(z)u(t) - x) \tag{34}$$

subject to the following boundary conditions

$$x(0,t) = 0,\ x(\pi,t) = 0,\ x(z,0) = x_0(z) \tag{35}$$

where x denotes the dimensionless rod temperature, z is the spatial coordinate along the axis of the rod, β_T denotes the dimensionless heat of reaction, γ denotes the dimensionless activation energy, β_U denotes the dimensionless heat-transfer coefficient, $u(t)$ denotes the magnitude of actuation, and $b(z)$ accounts for the spatial profile of the actuator. For the above system the spatial differential operator $\mathcal{A}$ in Eq. 1 takes the form

$$\mathcal{A}(x) = \frac{\partial^2 x}{\partial z^2} \tag{36}$$

and the nonlinear function $f(x)$ can be represented as

$$f(x) = \beta_T(e^{-\gamma/(1+x)} - e^{-\gamma}) - \beta_U x \tag{37}$$

Two different spatial distributions for the actuator were investigated. Initially, spatially distributed actuation with $b(z) = H(z - 0.3\pi) - H(z - 0.7\pi)$, where $H(\cdot)$ denotes the

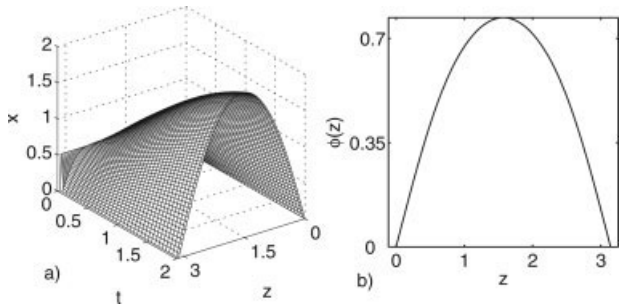

Figure 3. (a) Open loop profile of the state of the diffusion-reaction process with a linear spatial operator (Eq. 34) and (b) spatial profile of the dominant eigenfunction obtained from the initial ensemble of the system of Eq. 34.

standard Heaviside function, was considered. A point actuator was also considered, the actuator distribution function in this case being expressed by $b(z) = \delta(z - 0.4\pi)$, where $\delta(\cdot)$ denotes the modified Dirac function. The nominal values of the parameters are: $\beta_T = 16$, $\gamma = 2$, and $\beta_U = 2$. Figure 3a presents the evolution of the PDE for $u(t) = 0$ from an initial condition of $x(z, 0) = 0.5$. It can be observed that the system evolves away from the desired, spatially uniform, $x(z, t) = 0$ steady-state to another steady-state characterized by a non-uniform distribution of temperature across the rod, with the maximum reached at $z = \pi/2$. Hence, we conclude that the steady-state $x(z, t) = 0$ is an unstable one.

The control problem can be formulated as designing a state feedback controller that stabilizes the rod temperature to the spatially open-loop unstable steady-state. The controlled output $y_{c,i}$, is chosen to be the first dominant eigenmode (function $c(z)$ in Eq. 1 is chosen to be the first dominant eigenfunction) with a desired setpoint of $\hat{v} = 0$. We assume that the measurements of all the states of Eq. 34 are available and focus on state feedback control. The relative degree of the system r_i is one and the number of control inputs k, is one. The controller parameters used in Eq. 24 are $\beta_{11} = 1$ and $\beta_{10} = 0.95$.

Numerical results

In order to obtain a finite dimensional approximation of the infinite dimensional system of Eq. 34, initially an ensemble of 100 snapshots was generated for $u(t) = 0$. This has been presented in Figure 3a. Each snapshot is a spatial profile obtained at a fixed time instant from numerical simulations of Eqs. 34 and 35. The values of the discretized snapshot used were computed at 120 equispaced locations. Note that an exhaustive sampling of the state-space of the PDE for a number of different initial conditions and magnitudes of actuation was *not* required during the ensemble generation phase. Application of KLE at this initial stage resulted in a single dominant eigenfunction, which captured more than 99% of the energy embedded in the ensemble. This eigenfunction is shown in Figure 3b. Based on this eigenfunction a one-dimensional (1-D) reduced-order model was derived by applying Galerkin's method to the PDE system of Eqs. 34–35. Based on this system a feedback linearizing controller of the form of Eq. 25 was designed. During closed-loop process operation it was assumed that snapshots of the process evolution are available every $t_s = 0.1$ s. The finite dimensional process model and the control law were reconfigured after each new process measurement was received. In this work, the value of the user parameter ε was set to 99 i.e., the modes of the dominant subspace $\mathbb{P}$ captured at least 99% of the energy in the ensemble.

The process was initially simulated with spatially distributed actuation $b(z) = H(z - 0.3\pi) - H(z - 0.7\pi)$. Figure 4a presents the spatiotemporal profile of the rod temperature under closed-loop operation. We observe that the controller stabilizes the process at the open-loop unstable steady-state. Figure 4b presents the corresponding profile of the control action $u(t)$. We note that the control action $u(t)$ is a smooth function of time (i.e., the temporal profile exhibits no discontinuities or chattering), and converges to zero as the control objective is achieved. Even though more process measurements from the closed-loop operation were included in the ensemble, while simultaneously old snapshots were removed, one eigenfunction was found to capture 99% energy of the ensemble during the process evolution. This can be observed in Figure 4d; the percentage contribution of the dominant eigenvalue of c_q, ξ, in this case never increased to more than 1, and as a result, the subspace $\mathbb{P}$ was not augmented. The

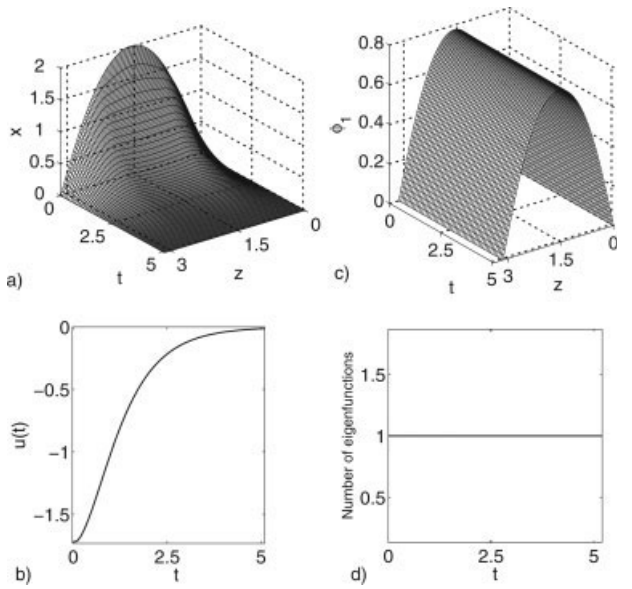

Figure 4. (a) Closed-loop temperature profile of the system of Eq. 34 using distributed actuation, $b(z) = H(z - 0.3\pi) - H(z - 0.7\pi)$ (b) temporal profile of control action using distributed actuation for the system of Eq. 34 (c) temporal profile of the dominant eigenfunction for the system of Eq. 34 when using distributed actuation and (d) temporal profile of the number of dominant empirical eigenfunctions used in the reduced-order ODE model Eq. 21 to capture the desired 99% energy of the ensemble.

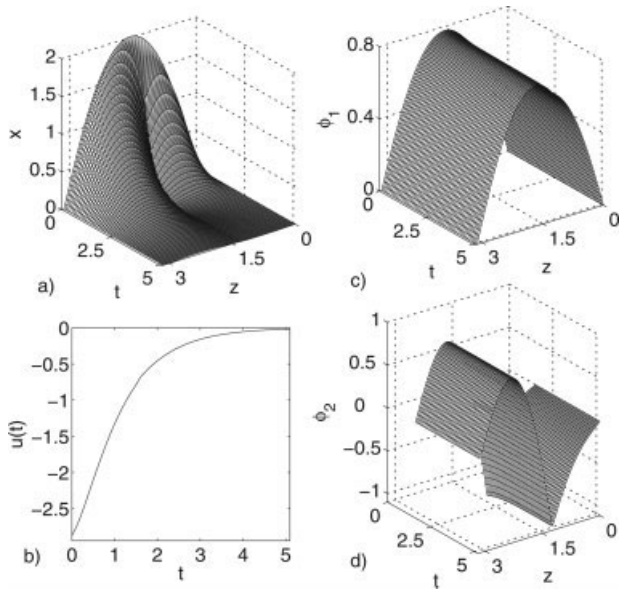

Figure 5. (a) Closed-loop temperature profile of the system of Eq. 34 using point actuation, $b(z) = \delta(z - 0.4\pi)$, (b) temporal profile of control action using point actuation, (c) temporal profile of the first dominant eigenfunction for the system of Eq. 34 using a point actuator, and (d) temporal profile of the second dominant eigenfunction for the system of Eq. 34.

dominant eigenfunction, however, was recomputed to account for the continuously changing ensemble of snapshots. The temporal profile of this dominant eigenfunction is presented in Figure 4c.

Subsequently, a point actuator $b(z) = \delta(z - 0.4\pi)$ was employed to control the same process with the same control objective. Figure 5a presents the spatiotemporal profile of the rod temperature under closed-loop operation. We observe that the controller successfully stabilizes the process at the open-loop unstable steady-state. Figure 5b presents the corresponding profile of the control action $u(t)$. We again observe that the control action is a smooth function of time; no discontinuities in the control action appear, and $u(t)$ approaches and remains at zero as the control objective is achieved. Figure 6a presents the temporal profile of the number of empirical eigenfunctions employed to obtain the reduced-order process model. As more process measurements from the closed-loop operation were included in the ensemble, while simultaneously old snapshots were removed, a new eigenfunction became dominant and joined the dominant eigenspace $\mathbb{P}$ at $t = 1.5$. Consequently, the dimensionality of the reduced-order ODE model was increased from $m = 1$ to $m = 2$. This can also be explicitly observed in Figure 6b, as ξ increased to more than 1%, the basis of subspace $\mathbb{P}$ was appended. The controller was reconfigured at this point based on the revised process model. In addition, the eigenfunctions were recomputed to account for the new trends appearing as the ensemble of snapshots was revised. The temporal profiles of these

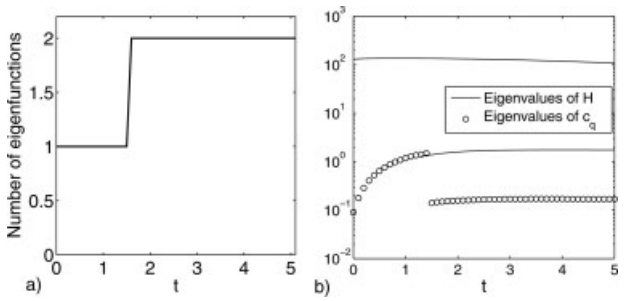

Figure 6. (a) Number of dominant empirical eigenfunctions used in the reduced-order model (Eq. 21) for the system of Eq. 34 as a function of time for point actuation $b(z) = \delta(z - 0.4\pi)$ and (b) temporal profiles of eigenvalues of H, and of the largest eigenvalue of c_q for the system of Eq. 34 using a point actuator.

two dominant eigenfunctions are presented in Figure 5c and d.

Spatially distributed actuation with nonlinear spatial operator and a spatially varying coefficient

In this section, we apply the proposed finite dimensional adaptive control method to the diffusion-reaction process considered in the previous section when the spatial differential operator is nonlinear (e.g., nonlinear dependence of thermal conductivity on temperature), and the dimensionless reaction rate constant β_T is spatially-varying. In this case, the process model is given by the following nonlinear parabolic PDE

$$\frac{\partial x}{\partial t} = \frac{\partial}{\partial z}\left(k(x)\frac{\partial x}{\partial z}\right) + \beta_T(z)(e^{-\gamma/(1+x)} - e^{-\gamma}) + \beta_U(b(z)u(t) - x) \quad (38)$$

subject to the following boundary conditions

$$x(0,t) = 0,\ x(\pi,t) = 0 \quad (39)$$

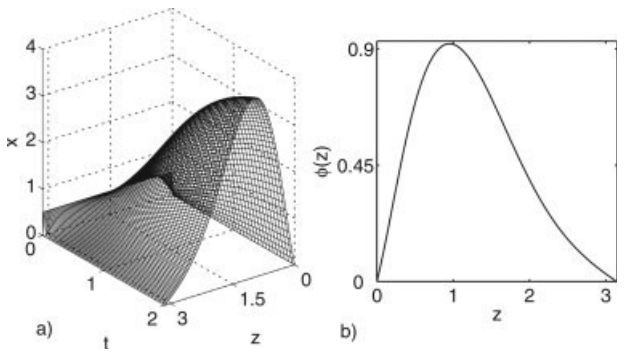

Figure 7. (a) Open loop profile of the state of the diffusion-reaction process with a nonlinear spatial operator (Eq. 38), and (b) spatial profile of the dominant eigenfunction obtained from the initial ensemble of the system of Eq. 38.

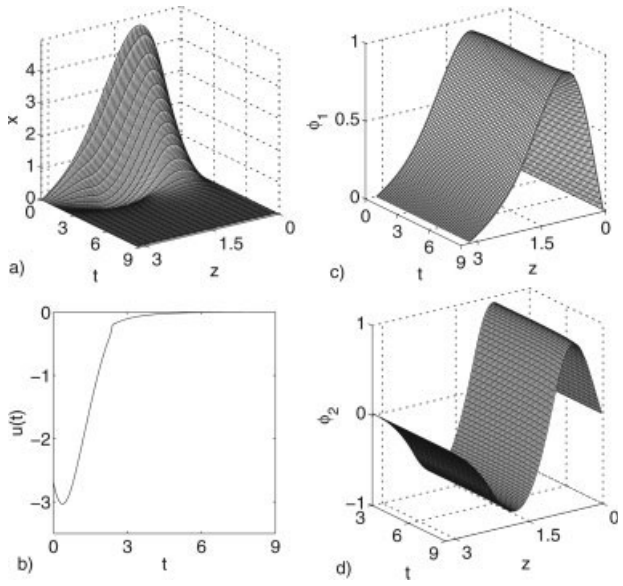

Figure 8. (a) Closed-loop temperature profile of the system of Eq. 38 using distributed actuation $b(z) = H(z - 0.3\pi) - H(z - 0.7\pi)$, (b) temporal profile of control action for the system Eq. 38, (c) temporal profile of the first dominant eigenfunction for the system of Eq. 38, and (d) temporal profile of the second dominant eigenfunction for the system of Eq. 38.

and the initial condition $x(z, 0) = x_0(z)$. $k(x)$ now is expressed by an explicit nonlinear function of the state, $\beta_T(z)$ denotes the dimensionless heat of reaction that is now an explicit function of the spatial coordinate z. The nominal values and expressions of the process parameters used in the presented simulations are: $k = 0.5 + 0.7/(x + 1)$, $x_0(z) = 0.5$, $\beta_T(z) = 16[\cos(z) + 1]$, $\gamma = 2$, and $\beta_U = 2$. The spatial differential operator $\mathcal{A}$ in Eq. 1 for the earlier process takes the form

$$\mathcal{A}(x) = \frac{\partial}{\partial z}\left(k(x)\frac{\partial x}{\partial z}\right) \tag{40}$$

and the nonlinear function $f(x)$ is of the form

$$f(x) = \beta_T(z)(e^{-\gamma/(1+x)} - e^{-\gamma}) - \beta_U x \tag{41}$$

Two different actuator cases were investigated. Initially, a spatially distributed actuation with $b(z) = H\ (z - 0.3\pi) - H\ (z - 0.7\pi)$ was considered and, subsequently, a point actuator $b(z) = \delta(z - 0.4\pi)$ was considered. Figure 7a presents the evolution of the PDE for $u(t) = 0$ from an initial condition of $x(z, t) = 0.5$. It can be observed that the operating steady-state $x(z, t) = 0$ is an unstable one, and the system converges to a stable spatially nonuniform steady state. The control problem is again formulated as designing a feedback controller that stabilizes the rod temperature at the above open-loop unstable steady-state.

Numerical results

We initially generated an ensemble of 100 snapshots of the infinite dimensional system of Eq. 38 with $u(t) = 0$, without performing an exhaustive sampling of the state-space of the PDE. This ensemble of snapshots has been presented in Figure 7a. Application of KLE along with the method of snapshots to this ensemble of snapshots resulted in a single dominant eigenfunction, which captured more then 99% of the energy embedded in the ensemble. This dominant eigenfunction is presented in Figure 7b.

We then simulated the process using spatially distributed actuation $b(z) = H(z - 0.3\pi) - H(z - 0.7\pi)$. Figure 8a presents the spatiotemporal profile of the rod temperature under closed-loop operation. We observe that the controller successfully stabilized the process at the open-loop unstable steady-state. Figure 8b presents the corresponding profile of the control action $u(t)$. We again note that the control action is a smooth function of time (with no discontinuities or chattering) and converges to zero as the control objective is achieved. Owing to nonsymmetric solution profile of Eq. 38, the number of empirical eigenfunctions required to capture 99% of energy of the ensemble changes from $m = 1$ to $m = 2$ at $t = 2.4$ (see Figure 9a). This can also be observed from Figure 9b; when ξ increased to more than 1%, the basis of subspace $\mathbb{P}$ was appended. In addition, the eigenfunctions were recomputed to account for the continuously changing ensemble of snapshots. This is demonstrated in Figure 8c and d which presents the temporal profiles of the two dominant eigenfunctions, respectively.

To investigate the applicability of the method when many modes are excited, and to illustrate the region of attraction of the closed-loop system for this case, we simulated the system (under the proposed controller) from uniform initial conditions of $x(z, 0) = 0.5$ and $x(z, 0) = -0.5$, respectively. Figure 10a presents the spatiotemporal profile of the rod temperature under closed-loop operation when starting from an initial condition of $x(z, 0) = 0.5$, and Figure 9b presents the spatiotemporal profile of the rod temperature when starting from an initial condition of $x(z, 0) = -0.5$. In both these simulations, the slow and the fast modes of the system are initially excited. Furthermore, we illustrate the fact that a previously captured ensemble of snapshots (we used an en-

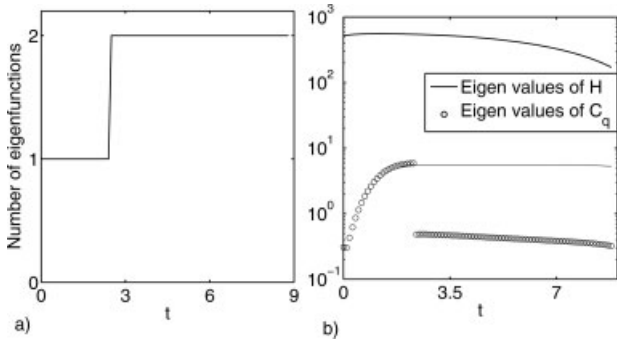

Figure 9. (a) Temporal profile of number of dominant empirical eigenfunctions used in the reduced-order model (Eq. 21) for the system of Eq. 38 (distributed actuation $b(z) = H(z - 0.3\pi) - H(z - 0.7\pi)$), and (b) temporal profiles of eigenvalues of H and of the largest eigenvalue of c_q for the system of Eq. 38 using a spatially distributed actuator.

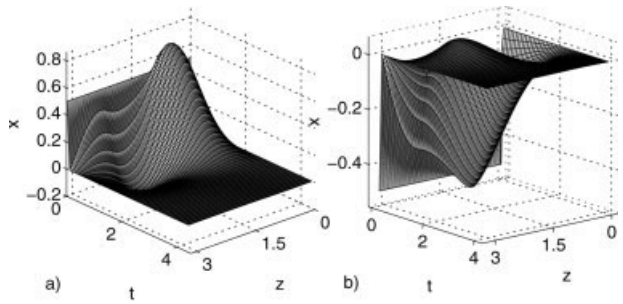

Figure 10. (a) Closed-loop temperature profile of the system of Eq. 38 for uniform initial condition of $x_0 = 0.5$ (distributed actuation, $b(z) = H(z - 0.3\pi) - H(z - 0.7\pi)$), and (b) closed-loop temperature profile of the system of Eq. 38 for a uniform initial condition of $x_0 = -0.5$ (distributed actuation).

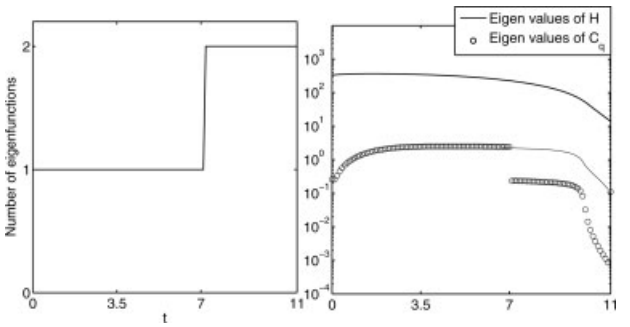

Figure 12. (a) Temporal profile of number of dominant empirical eigenfunctions used in the reduced-order model (Eq. 21), to capture the desired 99% of energy of the ensemble for the system of Eq. 38 (point actuation $b(z) = \delta(z - 0.4\pi)$), and (b) temporal profiles of eigenvalues of H and of the largest eigenvalue of c_q.

semble from a previous simulation run) can be used by our method. Using the "old ensemble" and the proposed method we observe that the closed-loop system successfully converges to the open-loop unstable steady-state in both cases.

We subsequently used a point actuator $b(z) = \delta(z - 0.4\pi)$ to simulate the aforementioned process. Figure 11a presents the spatiotemporal profile of the rod temperature under closed-loop operation. We again observe that the controller was successful in stabilizing the process at open-loop unstable steady-state. The profile of the computed control action is presented in Figure 11b. We observe that it is a smooth function of time and that it converges to zero. Figure 12a presents the variation in the number of empirical eigenfunctions employed to obtain the reduced-order process model. As more process measurements from the closed-loop operation were included in the ensemble while simultaneously old snapshots were removed, the percentage contribution ξ, of the dominant eigenvalue of c_q, increased to more than 1 (see Figure 12b), and, consequently, a new eigenfunction joined the dominant eigenspace at $t = 7.1$. The dimensionality of the reduced-order ODE model was at that time instant increased from $m = 1$ to $m = 2$. In addition, the eigenfunctions were recomputed to account for continuously changing ensemble of snapshots. The temporal profiles of these dominant eigenfunctions are presented in Figure 11c and d.

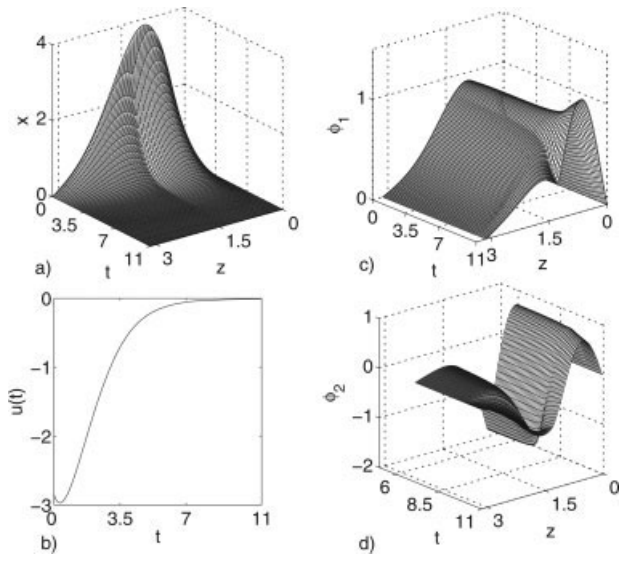

Figure 11. (a) Closed-loop temperature profile of the system of Eq. 38 using point actuator $b(z) = \delta(z - 0.4\pi)$, (b) temporal profile of control action, (c) temporal profile of the first dominant eigenfunction for the system of Eq. 38 when using a point actuator, and (d) temporal profile of the second dominant eigenfunctions for the system described by Eq. 38.

Effect of parametric uncertainty

To illustrate the effectiveness of the methodology under significant parametric uncertainty for the process described by Eq. 38, we assumed a 10% uncertainty in the process parameter $\beta_T(z)$, which leads to a more unstable open-loop process behavior. The nominal value of $\beta_T(z)$ was set at 17.6 $[\cos(z) + 1]$, and all the other process parameters were at the nominal values presented at the beginning of this section. The controller (Eq. 25), however, was designed using $\beta_T(z) = 16\ [\cos(z) + 1]$. We subsequently used a point actuator $b(z) = \delta(z - 0.4\pi)$ to simulate the aforementioned process. Figure 13a presents the spatiotemporal profile of the rod temperature under closed-loop operation. We observe that the controller stabilized the process at the open-loop unstable steady state even in the presence of 10% uncertainty in one of its process parameters (which is directly coupled to the nonlinear terms in Eq. 38). The computed control action was again a smooth function of time and no discontinuities or chattering appeared in its temporal profile. The temporal profile of this control action is presented in Figure 13b. Figure 14a, presents a temporal profile of the number of eigenfunctions employed to obtain the reduced-order process model (Eq. 21). A new eigenfunction joined the dominant eigen-

space at $t = 4.6$ when the percentage contribution ξ, of the dominant eigenvalue of c_q, increased to more than 1 (see Figure 14b). The second eigenfunction was removed from the dominant eigenspace at $t = 12.2$ when the corresponding eigenvalue of the first eigenfunction was found to capture the desired percentage (99%) of energy of ensemble. Figure 13c and d present the temporal profiles of the two eigenfunctions. It can be clearly observed that the eigenfunctions were recomputed to account for the continuously changing ensemble of snapshots.

Conclusions

This work extends the applicability of method of snapshots in the feedback control of dissipative PDE systems by relaxing the requirement for a large and representative ensemble of solutions, to cases where new snapshots become available during the process evolution, and as a result the ensemble of snapshots is continuously revised. The approach relies on the computation of an approximation of the eigenspace of the covariance matrix corresponding to its significant eigenvalues. This dominant eigenspace was updated recursively as new snapshots from the process are added to the ensemble, simultaneously increasing or decreasing its dimensionality if required. Under the assumption that the dimensionality of the dominant eigenspace remains small, the computational burden remained small implying that the methodology can be easily implemented online. The effectiveness of the proposed methodology was successfully demonstrated through representative examples of dissipative PDEs with both linear and nonlinear spatial differential operators. The methodology is being currently extended to cases where the availability of distributed sensors is restricted; output feedback controllers should then be designed. Specifically, snapshots of process become available only periodically and point measurements from a restricted number of sensors are continuously available.

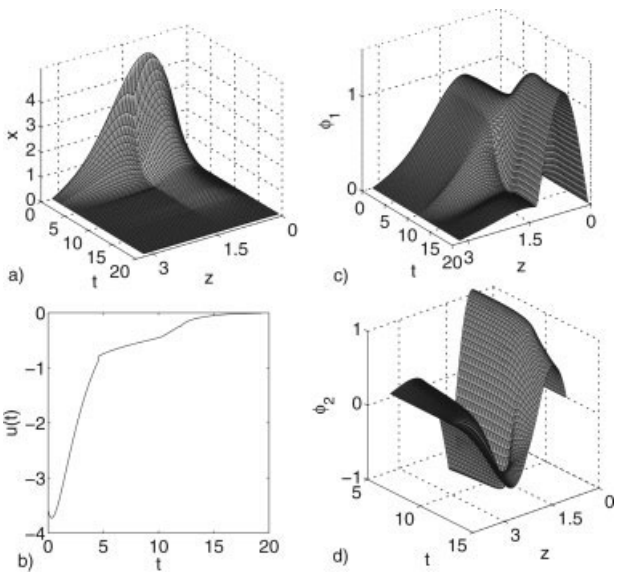

Figure 13. (a) Closed-loop temperature profile of the system of Eq. 38, using point actuator $b(z) = \delta(z - 0.4\pi)$ for 10% uncertainty in β_T, (b) temporal profile of control action, (c) temporal profile of the first dominant eigenfunction, and (d) temporal profile of the second dominant eigenfunction.

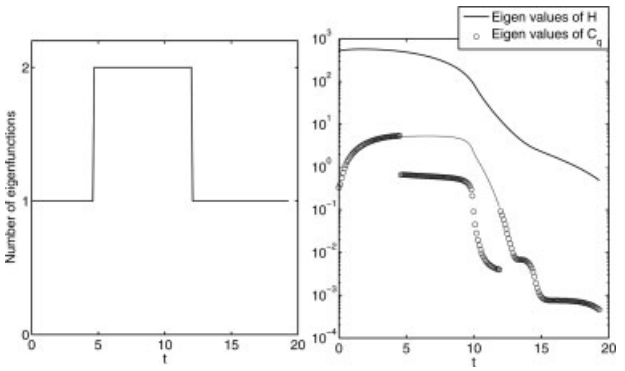

Figure 14. (a) Temporal profile of number of eigenfunctions of the system of Eq. 38 using point actuator $b(z) = \delta(z - 0.4\pi)$ for 10% uncertainty in β_T, and (b) temporal profiles of eigenvalues of H, and of the largest eigenvalue of c_q.

Literature Cited

1. Ray WH. *Advanced Process Control*. New York: McGraw-Hill; 1981.
2. Balas MJ. Feedback control of linear diffusion processes. *Int J Control*. 1979;29:523–533.
3. Balas MJ. Nonlinear finite-dimensional control of a class of nonlinear distributed parameter systems using residual-mode filters: A proof of local exponential stability. *J Math Anal Appl*. 1991;162:63–70.
4. Armaou A, Christofides PD. Wave suppression by nonlinear finite-dimensional control. *Chem Eng Sci*. 2000;55:2627–2640.
5. Armaou A, Christofides PD. Feedback control of the Kuramoto-Sivashinsky equation. *Physica D*. 2000;137:49–61.
6. Temam R. *Infinite-Dimensional Dynamical Systems in Mechanics and Physics*. New York: Springer-Verlag; 1988.
7. Foias C, Jolly MS, Kevrekidis IG, Sell GR, Titi ES. On the computation of inertial manifolds. *Phys Lett, A*. 1988;131:433–436.
8. Baker J, Christofides PD. Finite dimensional approximation and control of nonlinear parabolic PDE systems. *Int J Contr*. 2000;73:439–456.
9. Christofides PD, Daoutidis P. Finite-dimensional control of parabolic PDE systems using approximate inertial manifolds. *J Math Anal Appl*. 1997;216:398–420.
10. Titi ES. On approximate inertial manifolds to the navier-stokes equations. *J Math Anal Appl*. 1990;149:540–557.
11. Rathinam M, Petzold LR. A new look at proper orthogonal decomposition. *SIAM J Numen Anal*. 2003;41:1893–1925.
12. Homescu C, Petzold LR, Serban R. Error estimation for reduced-order models of dynamical systems. *SIAM Review*. 2007;49:277–299.
13. Sirovich L. Turbulence and the dynamics of coherent structures: part I, II and III. *Q Appl Math*. 1987;XLV:561–590.
14. Graham MD, Kevrekidis IG. Alternative approaches to the Karhunen-Loève decomposition for model reduction and data analysis. *Comp Chem Eng*. 1996;20:495–506.
15. Armaou A, Christofides PD. Dynamic optimization of dissipative PDE systems using nonlinear order reduction. *Chem Eng Sci*. 2002; 57:5083–5114.
16. Balsa-Canto E, Alonso AA, Banga JR. Reduced-order models for nonlinear distributed process systems and their application in dynamic optimization. *Ind Eng Chem Res*. 2004;43:3353–3363.

17. Balsa-Canto E, Banga JR, Alonso AA. A novel, efficient and reliable method for thermal process design and optimization. parts I and II. *J Food Eng*. 2002;52:227–247.
18. Shvartsman SY, Kevrekidis IG. Nonlinear model reduction for control of distributed parameter systems: a computer assisted study. *AICHE J*. 1998;44:1579–1595.
19. Alonso AA, Frouzakis CE, Kevrekidis IG. Optimal sensor placement for state reconstruction of distributed process systems. *AICHE J*. 2004;50:1438–1452.
20. Christofides PD. *Nonlinear and Robust Control of PDE Systems*. New York: Birkhäuser, 2000.
21. Bendersky E, Christofides PD. Optimization of transport-reaction processes using nonlinear model reduction. *Chem Eng Sci*. 2000;55: 4349–4366.
22. Holmes P, Lumley JL, Berkooz G. *Turbulence, Coherent Structures, Dynamical Systems and Symmetry*. Cambridge University Press; 1996.
23. Fukunaga K. *Introduction to statistical pattern recognition*. New York: Academic press; 1990.
24. Saad Y. *Iterative methods for sparse linear systems*. SIAM; 2003.
25. Kravaris C, Kantor JC. Geometric methods for nonlinear process control part 1 and 2. *Ind Eng Chem Res*. 1990;29:2295–2323.
26. Shroff GM, Keller HB. Stabilization of unstable procedurers: The Recursive Projection Method. *SIAM J Numer Anal*. 1993;30:1099–1120.

Appendix A

We note that the proof presented in this section is along the lines of the proof presented in Shroff and Keller.[26]

Lemma 1. The set of eigenvalues of $c_q = QC_KQ$ is the subset of eigenvalues of C_K that correspond to the eigenmodes which belong to subspace $\mathbb{Q}$.

Proof: Since C_K is symmetric and positive definite, there exists a real block diagonal decomposition of C_K

$$C_K = WJW^{-1} \tag{A1}$$

where

$$W = (W_1, W_2), \quad W_1 \in \mathbb{R}^{K\times m}, \quad W_2 \in \mathbb{R}^{K\times(K-m)} \tag{A2}$$

and

$$J = \begin{pmatrix} J_1 & 0 \\ 0 & J_2 \end{pmatrix}, \quad J_1 \in \mathbb{R}^{m\times m}, \quad J_2 \in \mathbb{R}^{(K-m)\times(K-m)} \tag{A3}$$

The columns of W_1 and W_2 form the bases for the subspaces associated with $\lambda_1, \ldots, \lambda_m$ and $\lambda_{m+1}, \ldots, \lambda_K$ respectively. The block J_1 is associated with the eigenvalues $\lambda_1, \ldots, \lambda_m$ and J_2 contains the block for $\lambda_{m+1}, \ldots, \lambda_K$. By definition the range space of W_1 is $\mathbb{P}$, which implies $QW_1 = 0$

$$C_KW_2 = W_2J_2 \tag{A4}$$

and

$$QW_2J_2 = QC_KW_2 = QC_K(PW_2 + QW_2) = QC_KQW_2 \tag{A5}$$

Here we used the fact that $QC_kP = 0$. (Since P is an orthogonal projector we know that $P^2 = P$. As a result we can write $C_KP = PC_KP$, and the result follows from the fact that $QP = 0$). Let $V = [W_1, QW_2]$, and use $Q^2 = Q$, $QW_1 = 0$ to get

$$QC_KQV = QC_kQ([W_1, QW_2]) = (W_1, QW_2)\begin{pmatrix} 0 & 0 \\ 0 & J_2 \end{pmatrix} \tag{A6}$$

Since W is nonsingular, it can be shown that V is also nonsingular

$$QC_KQ = V\begin{pmatrix} 0 & 0 \\ 0 & J_2 \end{pmatrix}V^{-1} \tag{A7}$$

Since the eigenvalues of J_2 are $\lambda_{m+1}, \ldots, \lambda_K$ is a subset of eigenvalues of C_K, the result follows.

Manuscript received Apr. 25, 2008, and revision received Oct. 23, 2008.